Large-Eddy Simulation of Sandia Flame D with Efficient Explicit Filtering

A. Bertels[1] · B. Kober[1] · A. Rittler[1] · A. Kempf[1] (ORCID)

Abstract
A uniform Gaussian filter has been applied explicitly to the LES conservation equations for mass, momentum and mixture to simulate a piloted non-premixed methane-air flame (Sandia Flame D). Using a basic property of exponential functions, the three dimensional Gaussian filter is decomposed into the product of three one dimensional filters, greatly reducing the cost of filtering. Seven simulations on three different grids have been performed to investigate the influence of grid refinement with a purely implicit filter, the effects of explicit filtering with increasing filter width and the effect of grid refinement at constant filter-size. Overall, consistent results have been achieved at a cost that is moderate with implicit or explicit filtering, so that explicit filtering can be applied in cases where the numerical error should be independent of the modelling error.

Keywords Large-eddy simulation · Non-premixed turbulent combustion · Sandia flame D · Explicit filtering · Gaussian filter

1 Introduction

Large-Eddy Simulation of Combustion has gained much attention in recent years, attaining excellent results and predictability for quite challenging cases [1–6]. However, some issues remain with the method, including cost, the definition of suitable boundary conditions, and difficulties in situations where detailed transport and chemistry must be resolved—for example for the study of knock or pollutant formation. Many of these issues have been discussed with Pope's ten questions to LES [7] already.

A point of criticism, which has been rarely addressed, is the fact that LES with implicit Schumann filtering [8] links modeling and numerics in such a close manner, that it is neither

✉ A. Kempf
andreas.kempf@uni-due.de

A. Bertels
amirhossein.bertels@gmail.com

1   Chair for Fluid Dynamics - Institute for Combustion and Gasdynamics (IVG),
University of Duisburg-Essen, Duisburg, Germany

possible to really distinguish numerical and modeling errors nor to discuss the quality of a numerical method and of a model separately. This has lead to situations where some groups even model the effects of turbulence through dedicated numerical discretization schemes, referring to the resulting technique as "implicit LES" or "MILES". In turn, other researchers have ended up combining eddy viscosity sub-grid models with relatively inaccurate numerical method (that are ubiquitous in most commercial codes due to their favourable robosity) with the result that filtering and dissipation are rather achieved by the numerical treatment than by the eddy-viscosity, leading to an approach that might by labelled as "implicitly implicit LES". Related to this issue is the wish of many researchers and practicians of having a method that can assess the quality of a given simulation, using only data from the simulation itself. Many methods of this kind have been proposed [9–11], tested and had their shortcomings pointed out [12, 13], often by the original developers themselves. A very common problem of such quality estimators occurs in the above mentioned situation, where dissipative numerics are combined with eddy viscosity models, so that most of the dissipation is achieved in the numerics, leading to a low eddy viscosity, falsely implying that even small eddies are resolved, whereas the actual quality of such a simulation is quite low. In the case of LES of combustion, a further problem occurs, as research codes will often apply non-dissipative schemes for the transport of momentum, but have to rely on upwind-biased schemes (e.g. TVD or QUICK) for the transport of scalars, leading to a "numerical Schmidt-number effect" that one would wish to avoid.

Many of the problems mentioned above may be addressed (at least partially) by applying explicit filtering to LES, instead of the implicit filtering that is common practice, following an idea by Schumann [8]. Explicit filtering is not a new idea and was commonly applied in the early days of LES development, typically for simulations of canonical flows like homogeneous, isotropic turbulence or turbulent boundary layers [14], often in combination with spectral codes [14, 15], where the filtering of fields can be applied effectively and without dissipating the larger scales. Nevertheless, finite volume simulations with explicit filtering have also been demonstrated [16]. Several works using explicit filtering suggest that the solution obtained might be a converged solution independent of grid-spacing and numerical methods [16–20], due to reducing the numerical errors. Radhakrishnan and Bellan [21] have shown that a solution of the large-eddy simulation of a compressible single-phase flow obtained by explicitly filtering the small-scale producing non-linear terms in the governing equations can be discretization-order independent if the mesh-size is small enough, while they observed that the solution from conventional LES (implicitly filtered) are always discretization-order dependent. They also have shown that for obtaining grid-spacing-independent results, different filter-grid ratio have to be applied, depending on the order of accuracy of the discretization. Gallagher and Sankaran [22] have recently conducted the first explicitly filtered flame LES for a reacting bluff-body stabilized premixed flame by using an explicitly filtered approach on a non-uniform grid and investigated the influence of explicit filtering on the large-scale structural changes to the flow field. They obtained a good grid independence for this approach especially for the mean quantities. A moving least squares method has been used in their work to compute the weights required for the filtering operation as a pre-processing step, greatly reducing the high cost that would otherwise result from explicit filtering on unstructured grids.

Related to explicit filtering are attempts of modelling the subgrid-contributions by "defiltering" or "deconvolution" based combustion models, which has recently been demonstrated by different authors, including Domingo and Vervisch [23]. In their work, the explicit inverse filter is derived from a Taylor expansion of well-defined (Gaussian) filtering operation. To compare the approximate three-dimensional fields against the exact ones, they

filtered a DNS database and then applied a deconvolution operator constructed from the topology-based SGS model. Another study related to deconvolution has been conducted by Wang and Ihme [24], who applied a regularized deconvolution method (RDM) based on a minimum mean square error optimization procedure to simulate a partially premixed flame. They have argued that the RDM can potentially be used as a closure model for turbulent combustion and can also compensate the drawbacks of approximate deconvolution methods regarding the boundedness and conservation of scalars.

In the LES of combustion, though, explicit filtering was rarely applied [22], probably due to the strong dependency of density on the thermo-chemical state and the resulting stability problems, due to the need for additional transport equations and models, due to the often complicated (realistic) burner geometries that need the highest possible resolution and probably due to the high cost of filtering, so that explicit filtering could rarely be afforded. In the present paper, we make an attempt to address these issues and present results from explicitly filtered LES in comparison to implicitly filtered simulations and the experimental data [25–27] for the well known "Flame D". In this test of explicitly filtered LES of combustion, we analyze how the independent variation of the grid and filter-size affects the results, how the results compare to an implicitly filtered LES, how the different variants behave in terms of computational cost, and what needs to be considered when applying the explicit filter to the momentum- and scalar-fields and to the boundary conditions.

Before discussing the method and our results, it seems appropriate to review the current state of the art of LES of combustion. Early simulations have been applied for purely premixed flames and are largely due to Menon, Fureby and Poinsot [28–30], and for purely non-premixed flames by Bushe, Forkel, Janicka, Jones, Kempf or Pitsch [5, 31–34]. Subsequent work has extended these simulations to partially premixed combustion, using extensions of the non-premixed and premixed models, but also flamelet generated manifolds and similar techniques [35], and even transported filtered density functions [36], linear eddy modeling [37], conditional moment closure [38], conditional source term estimation [39] and multiple mapping closures [40]. More recent developments of LES consider the combustion of liquid [41] and solid fuels, predict the formation of soot [42] and the synthesis of nano-particles [43, 44] and consider the effects of radiative heat transfer within the flame [45]. A common theme of all these simulations is the growing skill and complexity of the simulations—driven by progress in modeling, numerics, parallel programming and Moore's law [46] of exponentially growing computer power.

The present work, however, tries to demonstrate the feasibility of explicit LES filtering for combustion simulations and to evaluate and minimize its cost.

2 Experimental Setup

The piloted "Flame D" is a turbulent jet flame experimentally studied at Sydney University, Sandia National Laboratories and Darmstadt University [47]. The flame features a fuel jet, surrounded by a premixed pilot and an air co-flow. The fuel stream supplies a diluted mixture of 25% methane and 75% air (by volume) with a bulk velocity of $W_{jet} = 49.6$ m/s, Reynolds number $Re_{jet} \simeq 22,400$ and a jet diameter of $D = 7.2$ mm. The annular pilot burns a lean mixture (equivalence ratio = 0.77) of C_2H_2, H_2, air, CO_2 and N_2 and stabilizes the flame with a bulk velocity of $W_{pilot} = 11.4$ m/s, the laminar co-flow of air has a bulk velocity of $W_{co} = 0.9$ m/s. Further details of the experiment are provided by Barlow and Frank [25], Schneider et al. [48] and Masri et al. [49]. The flame has been a target of

the turbulent non-premixed flame workshop (TNF) [50] and has been simulated by many groups.

3 Modeling Approach

3.1 Filtering

Most of the turbulent kinetic energy exists in the large eddies that are resolved by LES, whereas smaller structures are removed by low-pass filtering, so that their effect on the large scales must be modeled. Filtering of a field ϕ is achieved by convolution with a filter kernel G_{3D}, resulting in the filtered field $\overline{\phi}$:

$$\overline{\phi(x, y, z)} = \iiint_{-\infty}^{\infty} G_{3D}(x-q, y-r, z-s)\, \phi(q, r, s)\, dq\, dr\, ds \tag{1}$$

In the present work, we use a Gaussian-filter with a filter-size $\widetilde{\Delta} = \varepsilon\Delta$, where ε is the filter-grid ratio and Δ is the cell-size, assuming an isotropic filter and cubic cells (as used in the present simulations):

$$G_{3D}(x, y, z) = \left(\frac{6}{\pi\widetilde{\Delta}^2}\right)^{3/2} \exp\left(-\frac{6}{\widetilde{\Delta}^2}(x^2 + y^2 + z^2)\right) \tag{2}$$

In the LES, the filter must be applied at each discrete point in three dimensions. The integral in Eq. 1 is discretized as the sum over all points within a "neighborhood" extending N points in each direction:

$$\overline{\phi(x^I, y^J, z^K)} \approx \Delta^3 \sum_{i=-N}^{N} \sum_{j=-N}^{N} \sum_{k=-N}^{N} G_{3D}(x^I - x^{I+i}, y^J - y^{J+j}, z^K - z^{K+k})\, \phi(x^{I+i}, y^{J+j}, z^{K+k}) \tag{3}$$

Equation 3 depends on the cell-spacing or cell-size Δ, which will be considerably smaller than the LES filter-width $\widetilde{\Delta}$ if explicit filtering is applied. The parameter N describing the size of the stencil must be chosen such that only "small" values of G_{3D} occur outside of the stencil. Setting $N = \varepsilon$ is normally sufficient for a good approximation of the integral since the Gaussian kernel approaches zero very fast outside of this range. This approximation is illustrated in Fig. 1 for two Gaussian kernels with different widths, where empty and filled circles represent the value of the Gaussian kernel at discrete cell centers in one dimensional physical space.

Evaluating Eq. 3 is a very costly operation, requiring $(2N + 1)^3$ multiplications at each grid-cell for every transport equation and time-step. For isotropic equidistant grids and filters, the cost can be reduced, using a technique that was also applied for generating turbulent inflow data for LES or DNS [51]. This technique requires to rewrite Eq. 2 as a product of one dimensional Gaussian-filters:

$$\begin{aligned}
G_{3D}(x, y, z) &= \left(\frac{6}{\pi\widetilde{\Delta}^2}\right)^{3/2} \exp\left(-\frac{6}{\widetilde{\Delta}^2}\left(x^2 + y^2 + z^2\right)\right) \\
&= C_1 \exp(C_2 x^2)\, \exp(C_2 y^2)\, \exp(C_2 z^2) \\
&= G_{1D}(x)\, G_{1D}(y)\, G_{1D}(z)
\end{aligned} \tag{4}$$
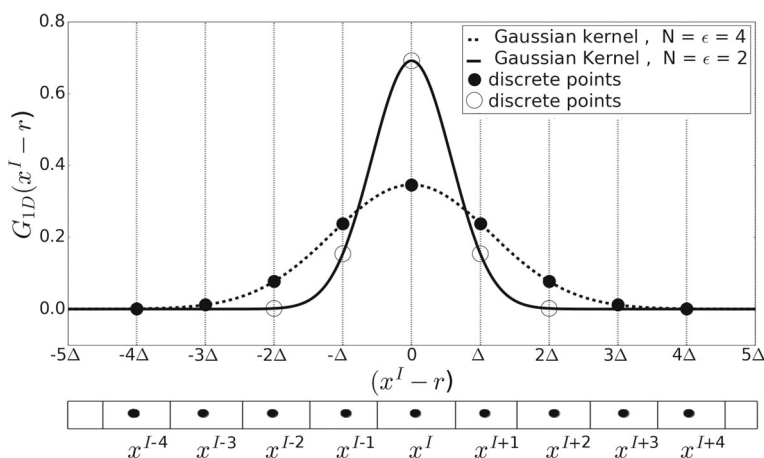
Fig. 1 Two Gaussian kernels with different widths, $\widetilde{\Delta} = 2\Delta$ and $\widetilde{\Delta} = 4\Delta$ respectively, where $\Delta = 1$ mm

As a result of Eq. 4, Eq. 3 can be written as:

$$
\begin{aligned}
\overline{\phi(x^I, y^J, z^K)} &\approx \Delta^3 \sum_{i=-N}^{N} \sum_{j=-N}^{N} \sum_{k=-N}^{N} G_{1D}(x^I - x^{I+i})\, G_{1D}(y^J - y^{J+j})\, G_{1D} \\
&\quad \times (z^K - z^{K+k})\, \phi(x^{I+i}, y^{J+j}, z^{K+k}) \\
&= \Delta^3 \sum_{i=-N}^{N} G_{1D}(x^I - x^{I+i}) \sum_{j=-N}^{N} G_{1D}(y^J - y^{J+j}) \\
&\quad \times \sum_{k=-N}^{N} G_{1D}(z^K - z^{K+k})\, \phi(x^{I+i}, y^{J+j}, z^{K+k})
\end{aligned}
\tag{5}
$$

Equation 5 can be interpreted (and implemented) as subsequent filtering in different directions: first, ϕ is filtered in direction z, the resulting field is then filtered in direction y, and this result is finally filtered in direction x, resulting in $\overline{\phi}$. This operation is far cheaper than the evaluation of Eq. 3—in fact, only $3(2N + 1)$ operations are required for each grid point, providing a potential speedup of $(2N + 1)^2/3$ or a factor of 27 for a realistic filter of size of $\widetilde{\Delta} = 4\Delta$.

3.2 Filtered governing equations

The Favre-filtered conservation equations for mass (ρ), momentum ($\rho\widetilde{u}_i$) and mixture ($\rho\widetilde{Z}$) are solved:

$$
\frac{\partial \overline{\rho}}{\partial t} + \frac{\partial \overline{\rho}\widetilde{u}_i}{\partial x_i} = 0
\tag{6}
$$

$$
\frac{\partial \overline{\rho}\widetilde{u}_i}{\partial t} + \frac{\partial \overline{\rho}\widetilde{u}_i\widetilde{u}_j}{\partial x_j} = \frac{\partial \overline{T}_{ij}}{\partial x_j} + \frac{\partial \overline{\rho}\tau_{ij}^{sgs}}{\partial x_j} - \frac{\partial \overline{p}}{\partial x_i}
\tag{7}
$$

$$
\frac{\partial \overline{\rho}\widetilde{Z}}{\partial t} + \frac{\partial \overline{\rho}\widetilde{Z}\widetilde{u}_i}{\partial x_i} = \frac{\partial}{\partial x_i}\left(\overline{\rho}D_S \frac{\widetilde{Z}}{\partial x_i}\right)
\tag{8}
$$

The above equations involve the filtered viscous stress tensor $\overline{T}_{ij}$ and the sub-grid stresses τ_{ij}^{sgs}. The unresolved turbulent fluxes are determined with an eddy diffusivity approach. The effective diffusivity D_S is the sum of the molecular D and turbulent diffusivity D_t, which is determined from the turbulent viscosity ν_t and the turbulent Schmidt number $D_t = \nu_t/Sc_t$, which is set to 0.7. An algebraic model is used to obtain turbulent viscosity $\mu_t = \bar{\rho}(C_m \widetilde{\Delta})^2 \mathcal{D}_m(\widetilde{u}_i)$, where the differential operator is modeled by Nicoud's σ model [52], the model constant C_m is set to 1.5.

3.3 Combustion modeling

Combustion is modeled with the steady flamelet approach [53]. A 1-D non-premixed flame is pre-computed with the chemistry library Cantera [54] for the GRI 3.0 mechanism [55]. The thermo-chemical data ϕ are determined a priori to the simulations and are stored as a function of the mixture fraction Z in a look-up table $\phi(Z)$. The table has equidistant steps $\Delta Z = 0.005$ in the mixture fraction space with 201 entries to enable a quick and simple table look-up. A unity Lewis number is assumed. In the LES framework, only the filtered mixture fraction is known and the sub-filter distributions remain unknown. In the presented work, it is assumed that the sub-filter distribution of the mixture fraction may be described by a top-hat (TH) filtered density function (FDF) [56] following Floyd et al. [56] or Olbricht et al. [57]. The SGS variances were modeled according to a gradient model, which leads to Eq. 9 with a constant C chosen as 0.25.

$$\widetilde{Z''^2} \simeq C \widetilde{\Delta}_i^2 \left(\frac{\partial \widetilde{Z}}{\partial x_i} \cdot \frac{\partial \widetilde{Z}}{\partial x_i} \right) \tag{9}$$

3.4 Numerical treatment

The numerical simulation is based on the in-house LES-code *PsiPhi* [58–61]. It solves the (incompressible) low-Mach number Favre-filtered equations based on a finite volume method (FVM) using a structured uniform equidistant orthogonal Cartesian grid. Continuity is enforced by a projection method, the corresponding Poisson equation for pressure is solved by the Gauss-Seidel method with successive over-relaxation (SOR). Parallelization is based on domain decomposition using the message passing interface (MPI) with non-blocking communication. The temporal discretization is performed by a low-storage third order Runge-Kutta scheme. Convective fluxes for momentum are discretized by a second order central differencing scheme, while a total variation diminishing (TVD) scheme has been applied for density and mixture. As inflow boundary conditions, the axial mean parabolic velocity profile as well as the inlet turbulent velocities as provided by Barlow et al. [47] have been set and the radial and tangential mean velocities were set to zero. Pseudo-turbulent velocity fluctuations were imposed at the inflow of the computational domain using Klein's artificial inflow generator [62] in a numerically efficient implementation [51], using the same efficient filter-decomposition as in the present work. A turbulent length scale of 1.5 mm has been used as estimated from the jet nozzle diameter. The mixture fraction is set to unity $Z = 1$ in the fuel nozzle, $Z = 0.27$ for the pilot and $Z = 0$ in the co-flow. Zero gradient boundary conditions were set for all transported quantities at the outlet, while negative normal velocities are clipped. Statistics are gathered after the simulations have reached a statistically-stationary state and are continued until at least 0.35 s (or 75 flow through times based on the jet bulk velocity). For the real times available in Table 2, FI

Table 1 Overview of the seven simulations

Cases	Δ [mm]	$\varepsilon = 1$	$\varepsilon = 2$	$\varepsilon = 4$
Coarse (C)	$\Delta_C = 0.5$	CI	–	–
Medium (M)	$\Delta_M = 0.25$	MI	M2	M4
Fine (F)	$\Delta_F = 0.125$	FI	F2	F4

The LES cell-size is denoted by Δ. The filter-grid ratio ε has been chosen as 1 (implicit filter), 2 and 4. The simulation on the coarsest grid is only feasible with implicit filtering

and F4 simulation requires 400,000 and 310,000 iterations respectively. Using 2,160 cores, these number of iterations correspond to 16 h and 39 min and 23 h and 37 min respectively.

For the explicitly filtered LES simulations, each time step t^n, the convective fluxes of momentum, density and mixture are explicitly filtered. The inflow momentum at each time step t^n is explicitly filtered in the inlet plane. The initial momentum, density and mixture fraction field over the whole computational domain are also explicitly filtered.

To investigate the influence of explicit filtering on the results, seven simulations for three different grid resolution as provided in Table 1 have been conducted. The coarse and medium runs use the same domain size, but a smaller size is used for the fine grid to keep the simulation affordable—following a previously tested strategy [63]. Each simulation is labeled by two characters, representing the resolution and the filter-grid ratio. For example, F4 represents a fine simulation with an explicit filter that is four times coarser than the grid cells. The implicitly filtered simulations can be seen as simulations with $\varepsilon = 1$, but are referred to as CI, MI and FI. The number of computational cells and the computational cost C are summarized in Table 2.

4 Results

The following section compares the results obtained from different simulations, using different combinations of filter- and cell size for simulating the flame, and for comparing the

Table 2 Mesh-size, filter-size, number of computational cells, physical simulation time, computational cost and normalized cost for the various simulations

Cases	Δ [mm]	$\widetilde{\Delta}$ [mm]	N_x	N_y	N_z	$\mathbf{n}_{cells}$ [10^6]	Real time [s]	Total cost C [10^3 Core hours]	Norm. cost C^* $\left[\frac{Core\ hours}{mm^3 s}\right]$
CI	0.5	0.5	120	120	450	6.5	1.6	7.0	0.005
MI	0.25	0.25	240	240	900	52	0.565	36	0.079
M2	0.25	0.5	240	240	900	52	0.672	51	0.094
M4	0.25	1.0	240	240	900	52	0.779	51	0.081
FI	0.125	0.125	240	240	900	52	0.415	36	0.857
F2	0.125	0.25	240	240	900	52	0.367	51	1.372
F4	0.125	0.5	240	240	900	52	0.383	51	1.315

The number of computational cells in axial and both lateral directions are given by N_z, N_y and N_x respectively. Please note that some simulations can be cheaper with a larger filter, as the resulting smoother fields lead to less work in the iterative pressure correction step

results to the experiments. Based on this comparison, there is no clear "best" or "most accurate approach", and the reasons are not clear at this point. It will however be apparent that the explicit filtering a) does affect the computational result, b) that such filtering is feasible, that c) filtering can potentially separate numerical and modelling errors, and that d) such filtering can be implemented in a stable, robust and cost-effective way.

Figure 2 shows how refining the grid from $\Delta_C = 0.5$ mm through $\Delta_M = 0.25$ mm to $\Delta_F = 0.125$ mm affects the resolution of the instantaneous temperature fields when implicit filtering is applied, i.e. when the cell-size is identified with the LES filter width. In turn, Fig. 3 shows how the resolution changes if the cell-size is maintained at Δ_F, but the filter-size is increased from $\widetilde{\Delta} = \Delta_F$ through $\widetilde{\Delta} = 2\Delta_F$ to $\widetilde{\Delta} = 4\Delta_F$ (with explicit filtering). In either case (Figs. 2 or 3), the change in resolution is apparent. Where these qualitative differences are very visible, a meaningful comparison of the different combinations of grid
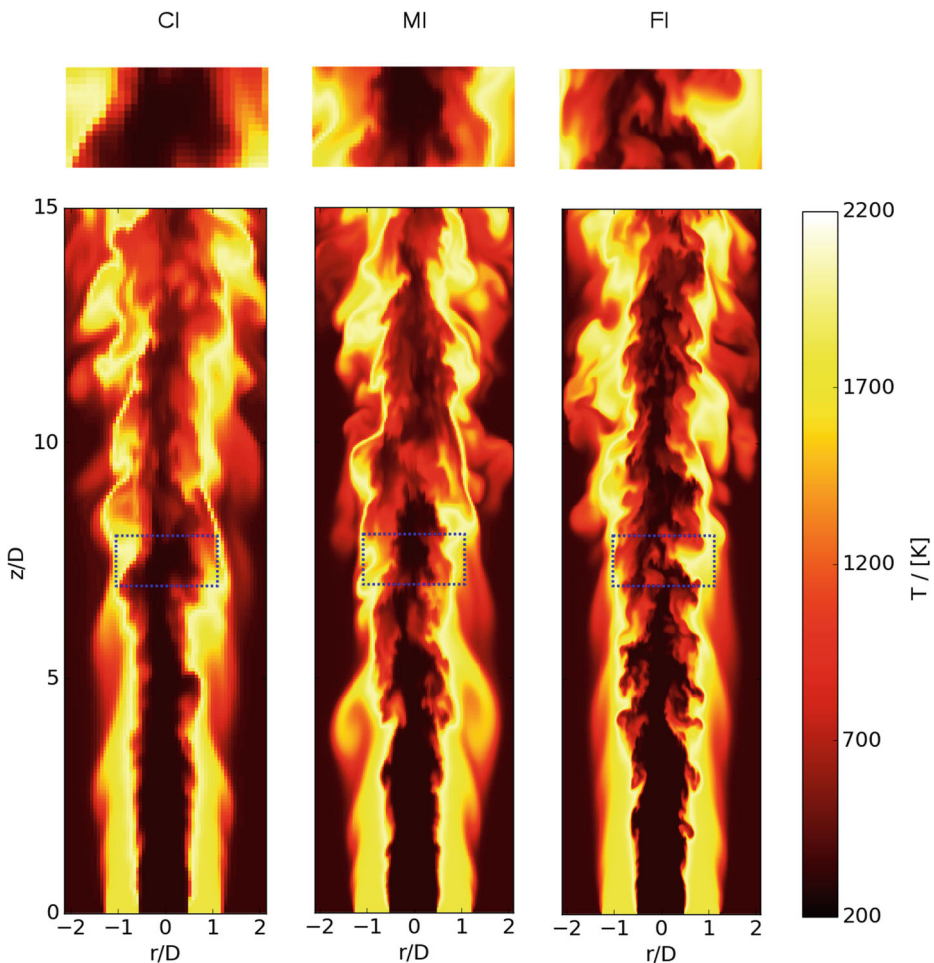
Fig. 2 Instantaneous plots of temperature in the burner mid-section for the three different grid resolutions coarse ($\Delta = 0.5$ mm), medium ($\Delta = 0.25$ mm) and fine ($\Delta = 0.125$ mm) with implicit filtering. The dashed regions of the plots are zoomed in at the top
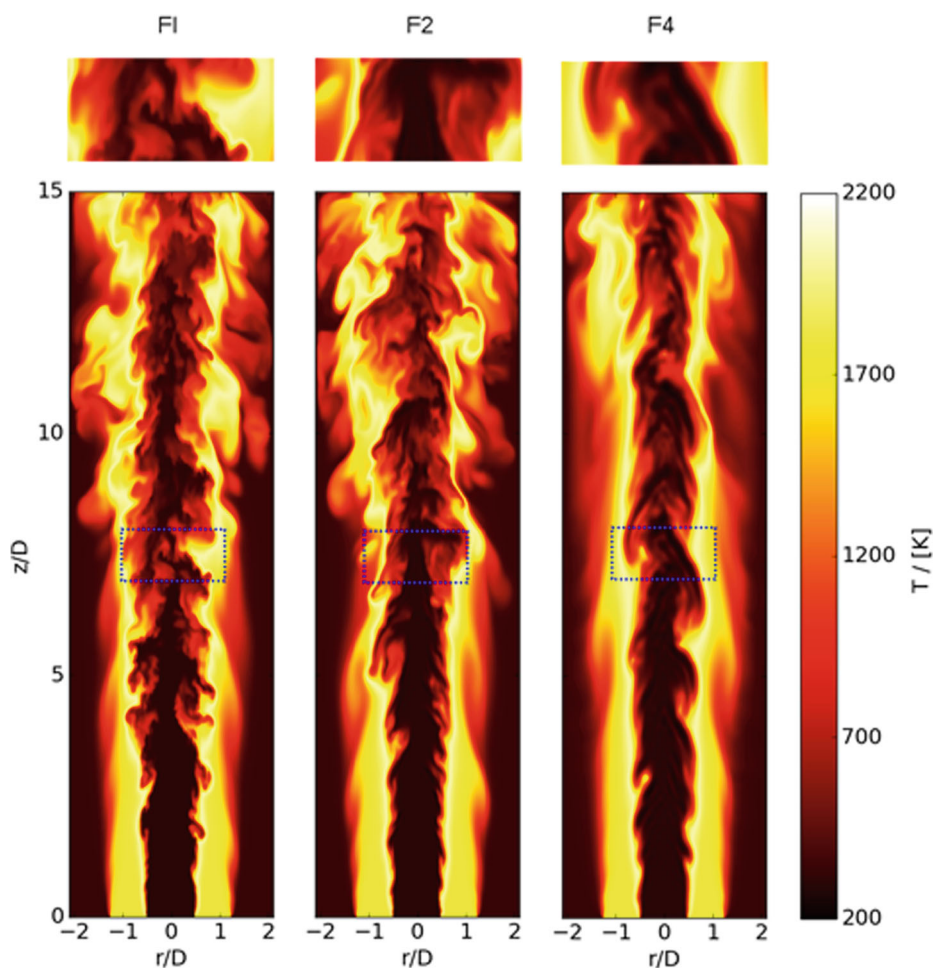
Fig. 3 Instantaneous plots of temperature in the burner mid-section for the three different filter widths **FI** ($\widetilde{\Delta} = 0.125$ mm), **F2** ($\widetilde{\Delta} = 0.25$ mm) and **F4** ($\widetilde{\Delta} = 0.5$ mm) on the fine grid. The dashed regions of the plots are zoomed in at the top

and filter size must consider the experimental evidence, typically for means and standard deviations of the velocity and scalar fields.

4.1 Coarsening with implicit LES

The first comparison illustrates how a classical coarsening of the grid will affect the predictions compared to the experiment when implicit filtering is used. (Please note that for the finest grid, data is only available to $z/D = 15$ to limit the computational cost). Figure 4 shows the evolution of the axial velocity W along the centerline—a quantity that agrees nicely with the measurements, already pointing to a good prediction of the jet spreading rate. The standard deviation W_{rms} of the axial velocity agrees reasonably well for axial locations greater than $15D$, but shows a considerable over-prediction near the nozzle. This is a
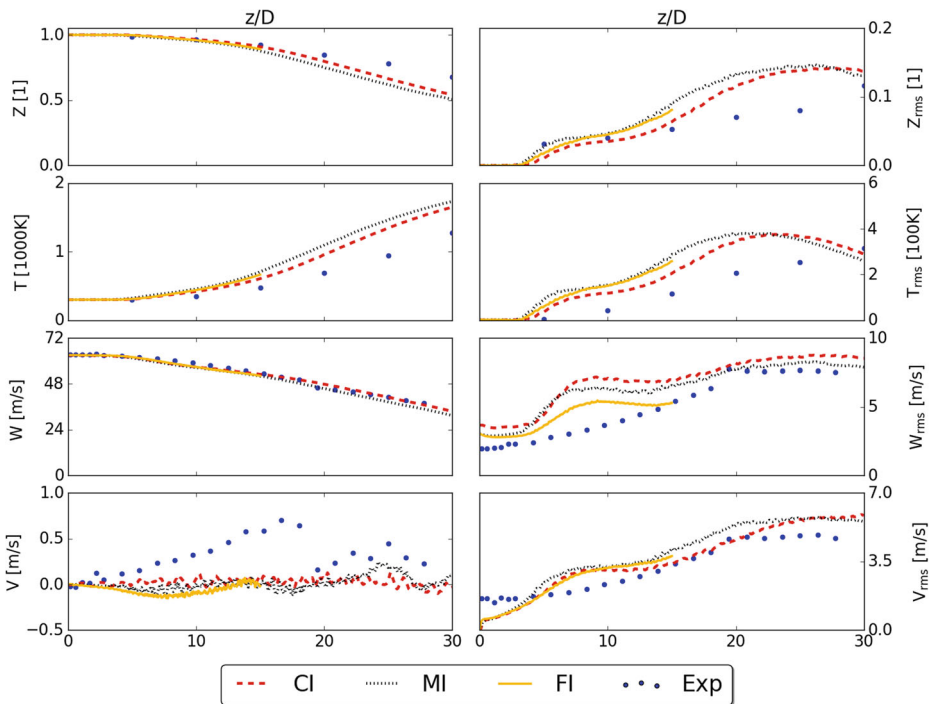
Fig. 4 Comparison of mean and fluctuation of axial profiles of mixture fraction, temperature, axial velocity and radial velocity for CI, MI and FI simulations

common problem in the incompressible large-eddy simulation of non-premixed jet flames that has been observed in several publications with different codes [63–65]. It is however apparent to what a large degree the mesh-refinement helps to improve the results to a more satisfactory level. Figure 4 also shows the radial velocity V, giving an impression of the error and asymmetry in the measurements. For the radial velocity fluctuation V_{rms}, one observes a much weaker grid-dependency and a better agreement than for the axial velocity fluctuation W_{rms}. As expected from the good agreement in the velocity field, the mean mixture fraction Z is also reasonably well predicted, but with a too lean mixture downstream of $15D$. This underestimated mean mixture fraction may explain why the mixture fraction fluctuation is considerably over-estimated in the downstream region, as the highest possible mixture fraction fluctuation is given as $Z_{rms}^2 < Z_{mean}(1 - Z_{mean})$. Finally, the temperature field shows an over-prediction of the mean temperature, which may again be explained by the mean mixture fractions that have been predicted too close to stoichiometry. Overall, the implicit filtering provides acceptable results along the centerline that are largely grid-independent, with the notable exception of the axial velocity fluctuation W_{rms}.

To obtain a better insight into the mixing and combustion away from the centerline, data is shown along different radial lines at $z/D = 1, 7.5, 15$ in Fig. 5. For the mixture fraction and temperature, the overall agreement seems good. A good agreement is also achieved for the temperature, showing some minor deviations on the finest grid at a larger radius, in a location that is relatively close to the lateral boundary of the computational domain (which is smallest for the fine grid to limit the computational cost). Finally, the prediction of the mean mass-fraction Y_{OH} of the hydroxyl radical is acceptable away from the nozzle. At
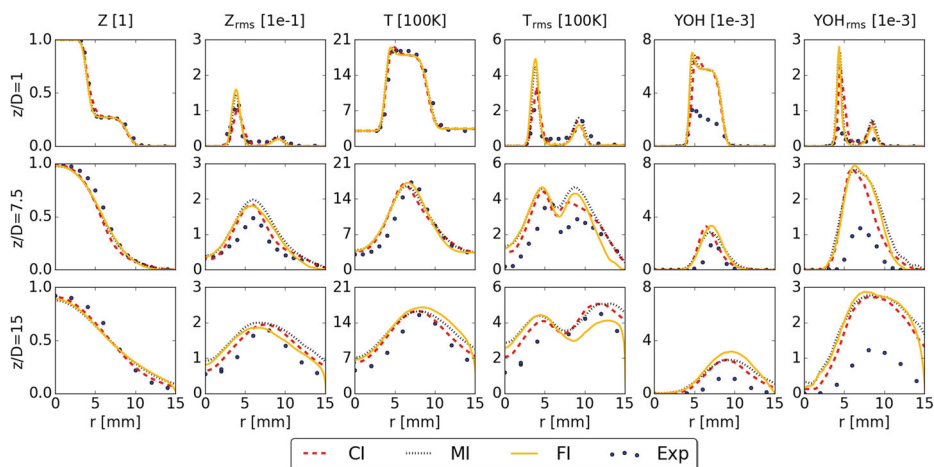
Fig. 5 Comparison of mean and fluctuation of radial profiles of mixture fraction, temperature and mass fraction of OH at different axial positions for CI, MI and FI simulations versus radius

$z = 1D$, the strong deviation is explained by the fact that the non-premixed flamelet is not well suited for the description of the premixed pilot flame, which is the only note-worthy heat-source this close to the burner. The fluctuations in the OH mass fraction are as expected from the prediction of the mean. Overall, the predictions of the first two statistical moments of mixture fraction and temperature are good, at least away from the center-line and the limits of the computational domain.

In summary, the implicit LES results presented show a satisfactory agreement with the experiments on all grids, with the exception of the axial velocity fluctuation, which has been identified as problematic before.

4.2 Filter-coarsening with explicit LES at fine grid resolution

The second comparison illustrates how coarsening the (explicit) filter will affect the predictions if the computational grid is kept constant. The case FI is identical to the finest case discussed in the previous section, so that the analysis can focus on the differences between this case and cases F2 and F4, with filter widths of $\widetilde{\Delta} = 2\Delta_F$ and $\widetilde{\Delta} = 4\Delta_F$ respectively. (Please note that for the fine grid, data is only available up to $z/D = 15$ due to the reduced domain size).

Figure 6 shows the axial evolution of the velocity and scalar fields. As for the implicitly filtered simulations, the mean axial velocity is predicted well. The explicit filtering does not appear to affect the results to a great extent, with the exception of the problematic axial velocity fluctuation W_{rms}, for which the local over-prediction is reduced if the largest explicit filter (F4) is applied. It has to be mentioned that both refining the grid (from CI to FI) and also explicit filtering (from FI to F4) can improve prediction of the axial velocity fluctuations along the centerline. Overall, both axial and radial velocity field are well captured by the simulations, which is a prerequisite for the prediction of the scalar quantities.

Figure 7 shows the radial profiles of the relevant scalars with a good overall agreement with measurements, showing very similar results for the cases with implicit filtering and mild explicit filtering, but a considerable difference with the large explicit filter—in particular away from the centerline. This difference is very visible for mixture fraction and
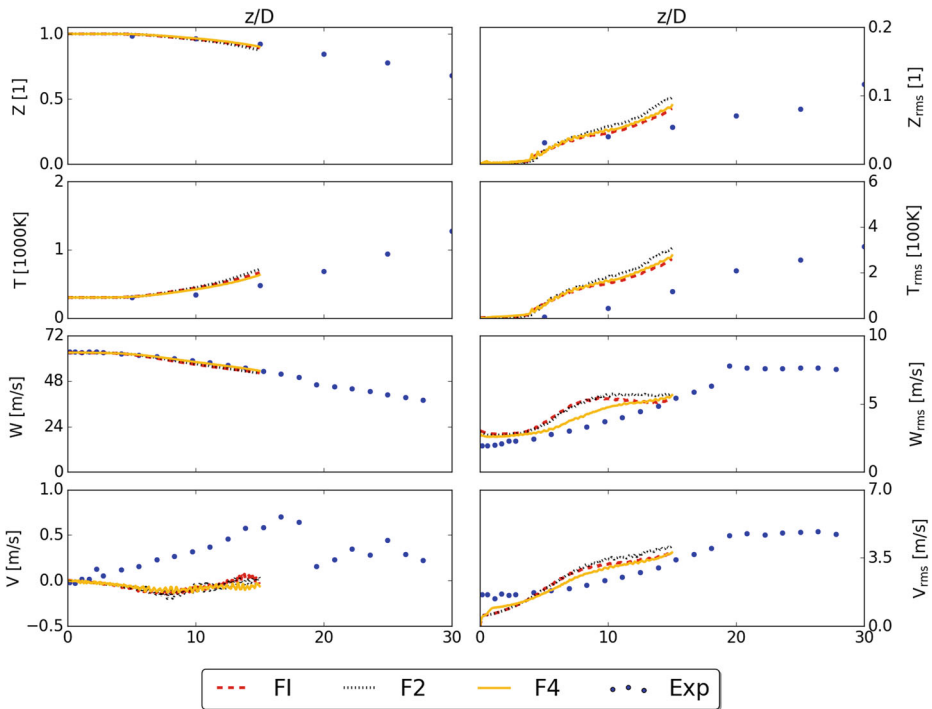
Fig. 6 Comparison of mean and fluctuation of axial profiles of mixture fraction, temperature, axial velocity and radial velocity for FI, F2 and F4 simulations

temperature fluctuations at downstream locations ($z/D = 7.5$ and $z/D = 15$), where filtering with the largest filter width (F4) can capture these fluctuations very well, especially away from the centerline, where mixing happens. Finally, explicit filtering does not seem to
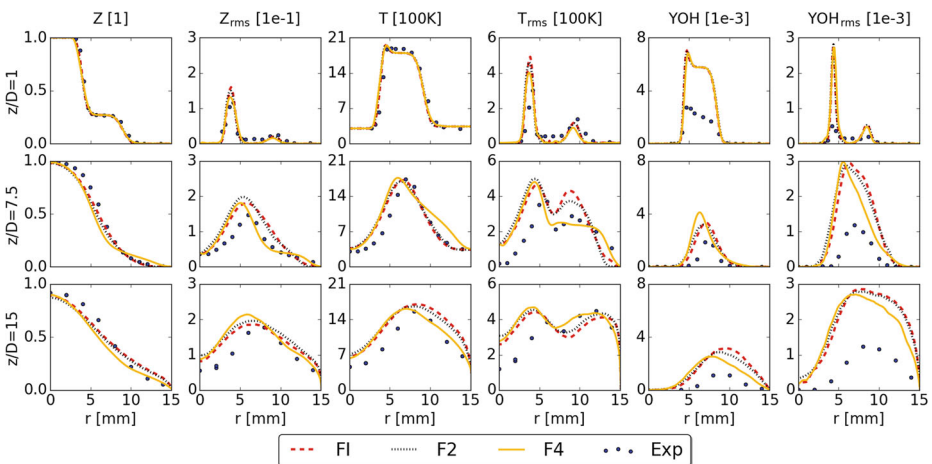

Fig. 7 Comparison of mean and fluctuation of radial profiles of mixture fraction, temperature and mass fraction of OH at different axial positions for FI, F2 and F4 simulations versus radius

improve the prediction of the mean and fluctuation of mass-fraction Y_{OH} of the hydroxyl radical by a great degree.

Overall, the explicit filtering with the largest filter-size can improve the fluctuation of the axial velocity on the centerline and also the fluctuation of the scalars in radial direction, where mixing plays an important role, by damping artificial fluctuations from the velocity and scalar fields.

4.3 Filter-coarsening with explicit LES at medium grid resolution

The previous study of filter-coarsening was conducted on a very fine grid and a short domain, this study is now repeated with a coarser grid and a longer domain. The effect of explicit filtering on the resolution of instantaneous temperature field is sketched in Fig. 8,
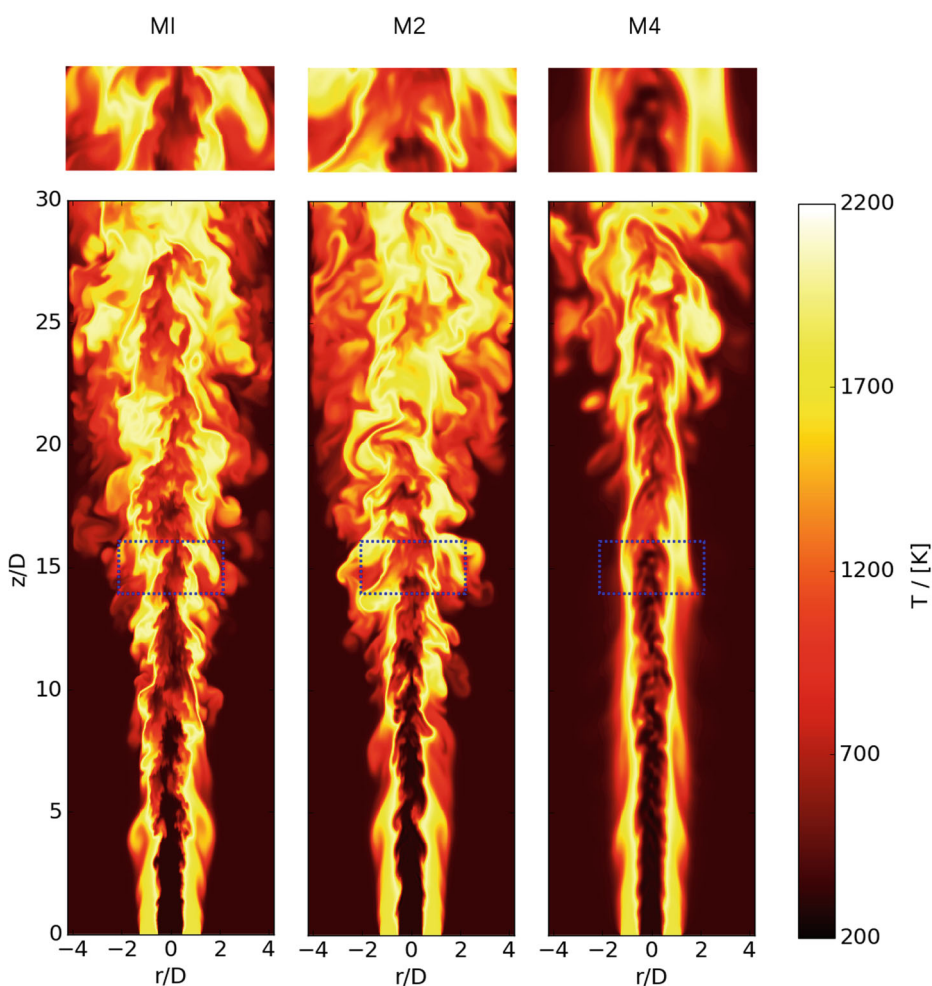

Fig. 8 Instantaneous plots of temperature in the burner mid-section for the three different filter widths **MI** ($\widetilde{\Delta} = 0.25$ mm), **M2** ($\widetilde{\Delta} = 0.5$ mm) and **M4** ($\widetilde{\Delta} = 1$ mm) on the medium grid. The dashed regions of the plots are zoomed in at the top

which like the explicit filtering on the fine mesh shown in Fig. 3, represents the reduction of resolution when the filter-size is increased from $\widetilde{\Delta} = \Delta_M$ through $\widetilde{\Delta} = 2\Delta_M$ to $\widetilde{\Delta} = 4\Delta_M$ for MI, M2 and M4 respectively.

On the medium grid resolution, the explicit filtering has a very visible impact on the solution over the centerline, especially on the fluctuations. In comparison to the experimental data given in axial direction represented in Fig. 9, a good agreement can be observed for the axial velocity W. However, it is notable that filtering with the largest filter-size (M4) improves the agreement of axial velocity fluctuation W_{rms}. The mean mixture fraction Z is accurately predicted from the nozzle exit up to roughly $z/D = 15$, but further downstream, mixture fraction is underestimated. The over-prediction of mean temperature might be related to this relatively poor prediction of mean mixture fraction.

As for the axial profiles, explicit filtering with the largest filter width has a strong effect on the solution, especially in the region away from the centerline. This intense dependency of LES statistics on the large filter width in radial direction is shown in Fig. 10. The turbulent viscosity and mixture fraction variance are highly dependent on the square of the filter-size, so that widening the filter width on the medium grid from $\widetilde{\Delta} = \Delta_M$ to $\widetilde{\Delta} = 2\Delta_M$ and from $\widetilde{\Delta} = \Delta_M$ to $\widetilde{\Delta} = 4\Delta_M$ should increase the turbulent viscosity and variance of mixture fraction 4 and 16 times respectively. This dependency of turbulent viscosity μ_t and the variance of mixture fraction Z_{var} on the filter width is illustrated in Fig. 11. As well as the high viscosity introduced to the problem, removing perturbations by filtering with a relatively large filter-size (M4) leads to producing less turbulence, which can shift the virtual origin of the jet downstream, which is (qualitatively) very visible from the instantaneous
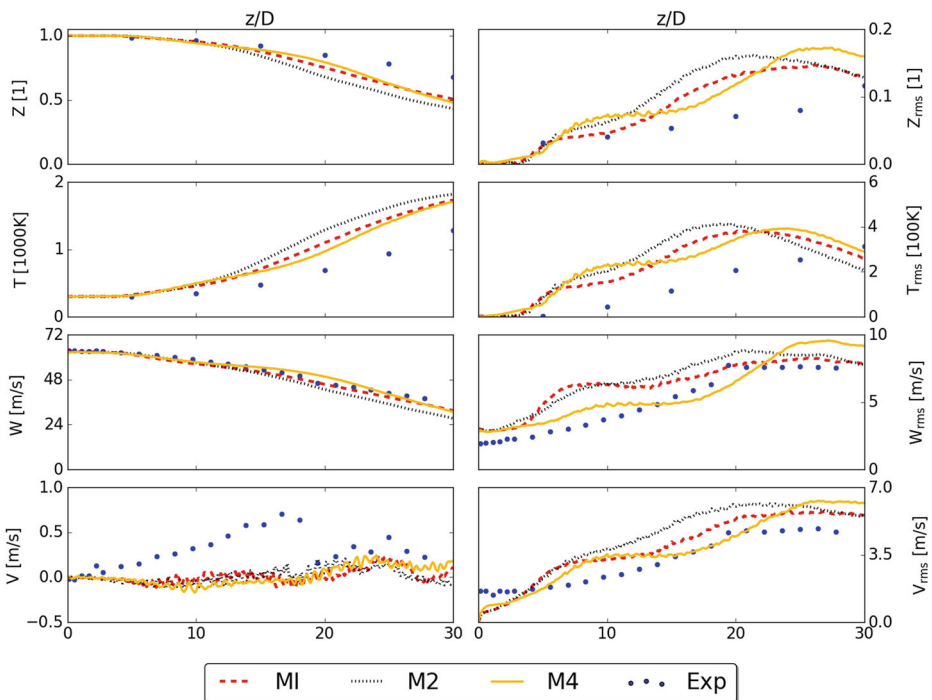
Fig. 9 Comparison of mean and fluctuation of axial profiles of mixture fraction, temperature, axial velocity and radial velocity for MI, M2 and M4 simulations
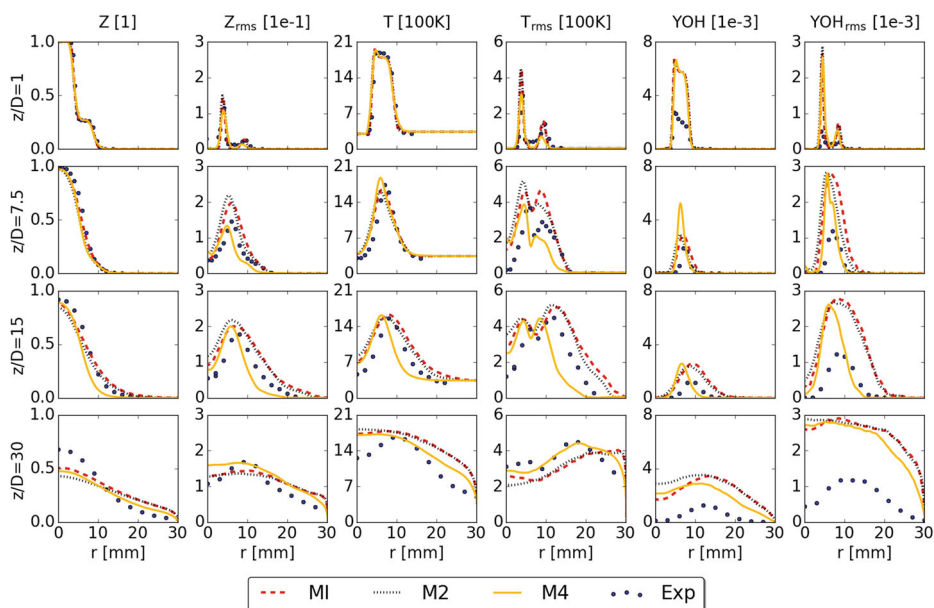
Fig. 10 Comparison of mean and fluctuation of radial profiles of mixture fraction, temperature and mass fraction of OH at different axial positions for MI, M2 and M4 simulations versus radius

temperature field shown in Fig. 8 for the M4 simulation in comparison with the implicitly and mildly explicitly filtered cases MI and M2.

4.4 Grid-coarsening with explicit LES at constant filter width

To get a better understanding of how the cell-size can influence the mean and fluctuation of scalars, while the filter-size ($\widetilde{\Delta} = 0.5$ mm) is fixed, the radial and axial plots are shown
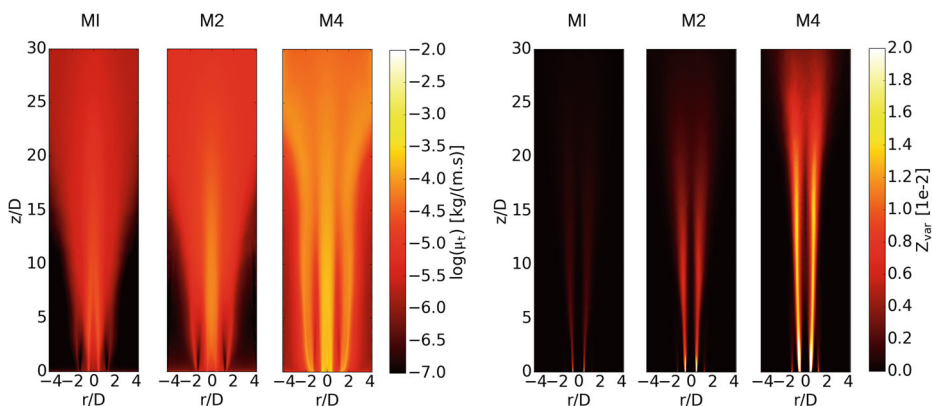
Fig. 11 The logarithm of turbulent viscosity (left) and the mixture fraction variance (right) of different simulations on the medium grid. The figure shows the severe influence of an increased filter width on turbulent viscosity and mixture fraction variance

in Figs. 13 and 12 respectively. Where the prediction of the velocity fluctuations improves steadily, mixture fraction and temperature fluctuations do not show such a "convergence". It is however worth to mention that explicitly filtering a simulation may require a finer grid than for an equivalent implicit simulation to resolve the smallest geometrical features of a case (Fig. 13).

4.5 Error analysis

At this point, the effect of explicit filtering has become apparent, but it is not possible to clearly state that it does improve results. Nevertheless, with the many comparisons presented above, it appears appropriate to compare the quality of the predictions, as measured by a global error measure. The root-mean-square error (RMSE) E is used, based on $Y^{(k)}$, which represents the quantity measured in the experiment and $\hat{Y}^{(k)}$, which denotes the same quantity computed in the simulation at the N_s available sampling points:

$$E = \sqrt{\frac{\sum_{k=1}^{N_s}(Y^{(k)} - \hat{Y}^{(k)})^2}{N_s}} \tag{10}$$

A low value of E denotes high accuracy. The errors are then normalized by the maximum error found for the corresponding quantity over the whole computational domain. The averaged errors for the mean and fluctuation of mixture fraction and temperature related to all test cases are given in Table 3. Perhaps disappointingly, there is no clear correlation of the
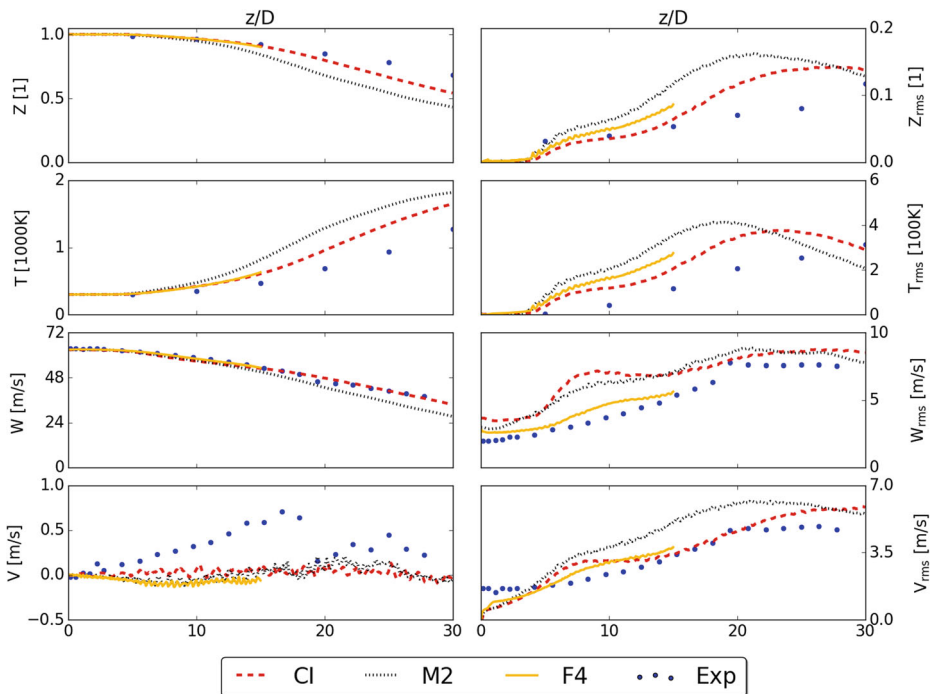
Fig. 12 Comparison of mean and fluctuation of axial profiles of mixture fraction, temperature, axial velocity and radial velocity for CI, M2 and F4 simulations
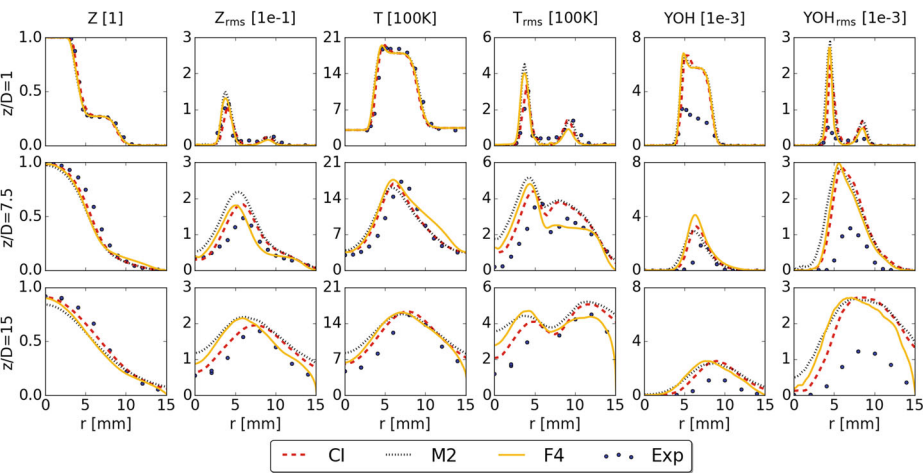
Fig. 13 Comparison of mean and fluctuation of radial profiles of mixture fraction, temperature and mass fraction of OH at different axial positions for CI, M2 and F4 simulations versus radius

error with the type of filtering, confirming that implicit filtering tends to work well most of the time, but also that explicit filtering can be applied (cost effectively) where needed.

4.6 Discussion

Large-eddy simulations of a flame have been presented, with explicit filtering. Interestingly, the explicit filtering has not shown the clear advantages that we would have hoped for— to some extend confirming that implicit filtering is a sensible approach. It is also possible that Sandia flame D is "too forgiving" for being a sufficiently challenging test-case for showing clear advantages (or disadvantageous) of explicit filtering. We will therefore conduct further testing for different flames in the future, and would encourage others to also do so—in particular for premixed combustion, thickened flame modelling or unstructured grids.

Table 3 The error E as defined in Eq. 10 for the mixture fraction and temperature means and standard deviations

Quantity	Case	$\varepsilon = 1$	$\varepsilon = 2$	$\varepsilon = 4$
$< Z >$	C	0.368		
	M	0.441	0.618	0.590
	F	0.350	0.426	0.486
$< T > [K]$	C	0.507		
	M	0.622	0.716	0.637
	F	0.549	0.604	0.607
Z_{rms}	C	0.405		
	M	0.550	0.654	0.469
	F	0.537	0.641	0.560
$T_{rms}[K]$	C	0.452		
	M	0.693	0.787	0.571
	F	0.739	0.829	0.725

Explicitly filtering the convective terms of the equations might lead to a quasi-reduction of Damköhler number and has an impact on the flame/turbulence interactions. However, it must be pointed out that at this point, there is no difference between explicit LES filtering and implicit LES filtering. For non-premixed flames, the turbulence model, the mixing models (turbulent diffusion here) and the reaction model (non-premixed flamelet here) are just kept, only the filter width in these models is adjusted. For premixed combustion with the common flame thickening, the thickening factor would have to be adjusted to correspond to the filter width, the wrinkling factor or efficiency function models would not need to change.

It is also interesting to note that with a non-premixed flamelet model (as used here), only the thermo-chemical state is obtained from the table as a function of mixture fraction and its subgrid-variance, whereas reaction source terms or heat release are not even known and could only be evaluated indirectly. It is however clear that explicit filtering will increase the size of the smallest features and hence the thickness of the mixing layers, and thus the amount of mixing and combustion that will have occurred at any point. This effect on heat release is, however, identical to the effect that implicit filtering with a coarsened grid will have—and is ideally compensated by the sub-grid model.

In order to compare the costs of explicit and implicit filtering, a non-dimensional cost $C^* = C/(V * t_r)$ has been introduced with the volume V of the computational domain and the real time t_r simulated, as presented in Table 2. This cost increases with explicit filtering by less than two. It is interesting to see that while the filtering with the larger filter (M4 and F4) takes more effort than with the smaller filter (M2 and F2), simulations with the larger filter are cheaper overall, which can be explained by the smoother fields resulting from the application of the wider filter, which require less iterations in the pressure correction step. Regarding the efficient filtering, the cost of normal (not efficient) filtering would be approximately 27 times higher (see Section 3.1), we estimate that a simulation with normal filtering would run approximately 13 times slower than one with efficient filtering or 24 times slower than one with implicit filtering. In other words, the cost-saving from efficient filtering is comparable to that of coarsening the grid (and time-step) by a factor of two in each direction.

5 Conclusions

Large-eddy simulations of a turbulent non-premixed flame have been presented, demonstrating that explicit filtering can be applied in a robust and cost-effective way, permitting reasonable predictions of experimental validation data. Consistent results have been achieved with both implicit and explicit filtering, where the additional cost of explicit filtering is moderate when the efficient filtering technique is applied. This opens up the possibility for combustion LES with explicit filtering, which can be considered as advantageous in any situation where the numerical error needs to be reduced independently of the modelling error introduced by filtering.

Compliance with Ethical Standards

Conflict of interest   There is no conflict of interest.

References

1. Domingo, P., Vervisch, L., Veynante, D.: Large-eddy simulation of a lifted methane jet flame in a vitiated coflow. Combust. Flame **152**(3), 415–432 (2008)
2. Fiorina, B., Mercier, R., Kuenne, G., Ketelheun, A., Avdić, A., Janicka, J., Geyer, D., Dreizler, A., Alenius, E., Duwig, C., et al.: Challenging modeling strategies for LES of non-adiabatic turbulent stratified combustion. Combust. Flame **162**(11), 4264–4282 (2015)
3. Gicquel, L.Y., Staffelbach, G., Poinsot, T.: Large eddy simulations of gaseous flames in gas turbine combustion chambers. Prog. Energy Combust. Sci. **38**(6), 782–817 (2012)
4. Jones, W., Prasad, V.: LES-pdf simulation of a spark ignited turbulent methane jet. Proc. Combust. Inst. **33**(1), 1355–1363 (2011)
5. Pitsch, H., Steiner, H.: Scalar mixing and dissipation rate in large-eddy simulations of non-premixed turbulent combustion. Proc. Combust. Inst. **28**(1), 41–49 (2000)
6. Stein, O., Olenik, G., Kronenburg, A., Marincola, F.C., Franchetti, B., Kempf, A., Ghiani, M., Vascellari, M., Hasse, C.: Towards comprehensive coal combustion modelling for LES. Flow Turbul. Combust. **90**(4), 859–884 (2013)
7. Pope, S.B.: Ten questions concerning the large-eddy simulation of turbulent flows. New J. Phys. **6**(1), 35 (2004)
8. Schumann, U., Sweet, R.A.: A direct method for the solution of poisson's equation with neumann boundary conditions on a staggered grid of arbitrary size. J. Comput. Phys. **20**(2), 171–182 (1976)
9. Celik, I., Klein, M., Freitag, M., Janicka, J.: Assessment measures for URANS/DES/LES: an overview with applications. J. Turbul. (7), N48 (2006)
10. Geurts, B.J., Fröhlich, J.: A framework for predicting accuracy limitations in large-eddy simulation. Phys. Fluids **14**(6), L41–L44 (2002)
11. Kempf, A., Lindstedt, R., Janicka, J.: Large-eddy simulation of a bluff-body stabilized nonpremixed flame. Combust. Flame **144**(1–2), 170–189 (2006)
12. Kempf, A.M., Geurts, B.J., Ma, T., Pettit, M., Stein, O.: Quality issues in combustion LES. J. Sci. Comput. **49**(1), 51–64 (2011)
13. Nguyen, T., Proch, F., Wlokas, I., Kempf, A.: Large eddy simulation of an internal combustion engine using an efficient immersed boundary technique. Flow Turbul. Combust. **97**(1), 191–230 (2016)
14. Gullbrand, J., Chow, F.K.: The effect of numerical errors and turbulence models in large-eddy simulations of channel flow, with and without explicit filtering. J. Fluid Mech. **495**, 323–341 (2003)
15. Jeanmart, H., Winckelmans, G.: Comparison of recent dynamic subgrid-scale models in turbulent channel flow. In: Proceedings of the Summer Program 2002, pp. 105–116 (2002)
16. Mathew, J., Lechner, R., Foysi, H., Sesterhenn, J., Friedrich, R.: An explicit filtering method for large eddy simulation of compressible flows. Phys. Fluids **15**(8), 2279–2289 (2003)
17. Bose, S.T., Moin, P., You, D.: Grid-independent large-eddy simulation using explicit filtering. Phys. Fluids **22**(10), 105,103 (2010)
18. Lund, T.: The use of explicit filters in large eddy simulation. Comput. Math. Appl. **46**(4), 603–616 (2003)
19. Radhakrishnan, S., Bellan, J.: Explicit filtering to obtain grid-spacing-independent and discretization-order-independent large-eddy simulation of two-phase volumetrically dilute flow with evaporation. J. Fluid Mech. **719**, 230–267 (2013)
20. Radhakrishnan, S., Bellan, J.: Explicitly-filtered LES for the grid-spacing-independent and discretization-order-independent prediction of a conserved scalar. Comput. Fluids **111**, 137–149 (2015)
21. Radhakrishnan, S., Bellan, J.: Explicit filtering to obtain grid-spacing-independent and discretization-order-independent large-eddy simulation of compressible single-phase flow. J. Fluid Mech. **697**, 399–435 (2012)
22. Gallagher, T.P., Sankaran, V.: Explicitly filtered LES of Bluff Body Stabilized Flames. In: 2018 AIAA Aerospace Sciences Meeting, p. 0441 (2018)
23. Domingo, P., Vervisch, L.: DNS and approximate deconvolution as a tool to analyse one-dimensional filtered flame sub-grid scale modelling. Combust. Flame **177**, 109–122 (2017)
24. Wang, Q., Ihme, M.: Regularized deconvolution method for turbulent combustion modeling. Combust. Flame **176**, 125–142 (2017)
25. Barlow, R., Frank, J.: Effects of turbulence on species mass fractions in methane/air jet flames. Proc. Combust. Inst. **27**(1), 1087–1095 (1998)
26. Cabra, R., Myhrvold, T., Chen, J., Dibble, R., Karpetis, A., Barlow, R.: Simultaneous laser Raman-Rayleigh-LIF measurements and numerical modeling results of a lifted turbulent H2/N2 jet flame in a vitiated coflow. Proc. Combust. Inst. **29**(2), 1881–1888 (2002)

27. Wegner, B., Maltsev, A., Schneider, C., Sadiki, A., Dreizler, A., Janicka, J.: Assessment of unsteady RANS in predicting swirl flow instability based on LES and experiments. Int. J. Heat Fluid Flow **25**(3), 528–536 (2004)

28. Menon, S., Calhoon, W.H.: Subgrid mixing and molecular transport modeling in a reacting shear layer. In: Symposium (International) on Combustion, vol. 26, pp. 59–66. Elsevier (1996)

29. Möller, S.I., Lundgren, E., Fureby, C.: Large eddy simulation of unsteady combustion. In: Symposium (International) on Combustion, vol. 26, pp. 241–248. Elsevier (1996)

30. Poinsot, T.: Using direct numerical simulations to understand premixed turbulent combustion. In: Symposium (International) on Combustion, vol. 26, pp. 219–232. Elsevier (1996)

31. Bushe, W.K., Steiner, H.: Conditional moment closure for large eddy simulation of nonpremixed turbulent reacting flows. Phys. Fluids **11**(7), 1896–1906 (1999)

32. Forkel, H., Janicka, J.: An efficient method for large-eddy simulation of turbulent diffusion flames. In: Proceedings of the Joint Meeting of the British, German and French Sections, pp. 53–55 (1999)

33. Jones, W., Kakhi, M.: PDF modeling of finite-rate chemistry effects in turbulent nonpremixed jet flames. Combust. Flame **115**(1–2), 210–229 (1998)

34. Kempf, A., Forkel, H., Chen, J.Y., Sadiki, A., Janicka, J.: Large-eddy simulation of a counterflow configuration with and without combustion. Proc. Combust. Inst. **28**(1), 35–40 (2000)

35. Oijen, J.v., Goey, L.d.: Modelling of premixed laminar flames using flamelet-generated manifolds. Combust. Sci. Technol. **161**(1), 113–137 (2000)

36. Raman, V., Pitsch, H., Fox, R.O.: Hybrid large-eddy simulation/lagrangian filtered-density-function approach for simulating turbulent combustion. Combust. Flame **143**(1–2), 56–78 (2005)

37. McMurthy, P.A., Menon, S., Kerstein, A.R.: A linear eddy sub-grid model for turbulent reacting flows: Application to hydrogen-air combustion. In: Symposium (International) on Combustion, vol. 24, pp. 271–278. Elsevier (1992)

38. Navarro-Martinez, S., Kronenburg, A., Di Mare, F.: Conditional moment closure for large eddy simulations. Flow Turbul. Combust. **75**(1–4), 245–274 (2005)

39. Steiner, H., Bushe, W.: Large eddy simulation of a turbulent reacting jet with conditional source-term estimation. Phys. Fluids **13**(3), 754–769 (2001)

40. Kronenburg, A., Cleary, M.: Multiple mapping conditioning for flames with partial premixing. Combust. Flame **155**(1–2), 215–231 (2008)

41. Rittler, A., Proch, F., Kempf, A.M.: LES of the sydney piloted spray flame series with the PFGM/ATF approach and different sub-filter models. Combust. Flame **162**(4), 1575–1598 (2015)

42. Bisetti, F., Blanquart, G., Mueller, M.E., Pitsch, H.: On the formation and early evolution of soot in turbulent nonpremixed flames. Combust. Flame **159**(1), 317–335 (2012)

43. Rittler, A., Deng, L., Wlokas, I., Kempf, A.: Large eddy simulations of nanoparticle synthesis from flame spray pyrolysis. Proc. Combust. Inst. **36**(1), 1077–1087 (2017)

44. Sung, Y., Raman, V., Fox, R.O.: Large-eddy-simulation-based multiscale modeling of TiO2 nanoparticle synthesis in a turbulent flame reactor using detailed nucleation chemistry. Chem. Eng. Sci. **66**(19), 4370–4381 (2011)

45. Rieth, M., Clements, A., Rabaçal, M., Proch, F., Stein, O., Kempf, A.: Flamelet LES modeling of coal combustion with detailed devolatilization by directly coupled CPD. Proc. Combust. Inst. **36**(2), 2181–2189 (2017)

46. Moore, G.E.: Cramming more components onto integrated circuits. Proc. IEEE **86**(1), 82–85 (1998)

47. Barlow, R., Frank, J.: Piloted CH4/Air flames C, D, E, and F–Release 2.1 15-JUN-2007. http://www.sandia.gov/TNF/DataArch/FlameD/SandiaPilotDoc21.pdf

48. Schneider, C., Dreizler, A., Janicka, J., Hassel, E.: Flow field measurements of stable and locally extinguishing hydrocarbon-fuelled jet flames. Combust. Flame **135**(1–2), 185–190 (2003)

49. Masri, A., Dally, B., Barlow, R., Carter, C.: The structure of the recirculation zone of a bluff-body combustor. In: Symposium (International) on Combustion, vol. 25, pp. 1301–1308. Elsevier (1994)

50. Barlow, R.: Turbulent non-premixed flame workshop. http://www.sandia.gov/TNF/abstract.html (2018)

51. Kempf, A.M., Wysocki, S., Pettit, M.: An efficient, parallel low-storage implementation of Klein's turbulence generator for LES and DNS. Comput. Fluids **60**, 58–60 (2012)

52. Nicoud, F., Toda, H.B., Cabrit, O., Bose, S., Lee, J.: Using singular values to build a subgrid-scale model for large eddy simulations. Phys. Fluids **23**(8), 085,106 (2011)

53. Peters, N.: Turbulent Combustion. Cambridge University Press, Cambridge (2000)

54. Goodwin, D.G.: Cantera. http://code.google.com/p/cantera (2009)

55. Smith, G.P., Golden, D.M., Frenklach, M., Moriarty, N.W., Eiteneer, B., Goldenberg, M., Bowman, C.T., Hanson, R.K., Song, S., Gardiner, W.C. Jr., Lissianski, V.V., Qin, Z.: http://www.me.berkeley.edu/gri_mech (2000)

56. Floyd, J., Kempf, A.M., Kronenburg, A., Ram, R.H.: A simple model for the filtered density function for passive scalar combustion LES. Combust. Theory Mod. **13**(4), 559–588 (2009)
57. Olbricht, C., Stein, O.T., Janicka, J., van Oijen, J.A., Wysocki, S., Kempf, A.M.: LES of lifted flames in a gas turbine model combustor using top-hat filtered PFGM chemistry. Fuel **96**, 100–107 (2012)
58. Inanc, E., Nguyen, M., Kaiser, S., Kempf, A.: High-resolution LES of a starting jet. Comput. Fluids **140**, 435–449 (2016)
59. Kempf, A., Geurts, B.J., Oefelein, J.: Error analysis of large-eddy simulation of the turbulent non-premixed sydney bluff-body flame. Combust. Flame **158**(12), 2408–2419 (2011)
60. Proch, F., Domingo, P., Vervisch, L., Kempf, A.M.: Flame resolved simulation of a turbulent premixed bluff-body burner experiment. Part I: analysis of the reaction zone dynamics with tabulated chemistry. Combust. Flame **180**, 321–339 (2017)
61. Rieth, M., Kempf, A., Kronenburg, A., Stein, O.: Carrier-phase DNS of pulverized coal particle ignition and volatile burning in a turbulent mixing layer. Fuel **212**, 364–374 (2018)
62. Klein, M., Sadiki, A., Janicka, J.: A digital filter based generation of inflow data for spatially developing direct numerical or large eddy simulations. J. Comput. Phys. **186**, 652–665 (2003)
63. Kempf, A., Sadiki, A., Janicka, J.: Prediction of finite chemistry effects using large eddy simulation. Proceedings of the Combustion Institute **29**(2), 1979–1985 (2002)
64. Kempf, A., Flemming, F., Janicka, J.: Investigation of lengthscales, scalar dissipation, and flame orientation in a piloted diffusion flame by LES. Proc. Combust. Inst. **30**(1), 557–565 (2005)
65. Renfro, M.W., Chaturvedy, A., King, G.B., Laurendeau, N.M., Kempf, A., Dreizler, A., Janicka, J.: Comparison of OH time-series measurements and large-eddy simulations in hydrogen jet flames. Combust. Flame **139**(1–2), 142–151 (2004)